A BEAM-SYNCHRONOUS GATED PEAK-DETECTOR FOR THE LHC BEAM OBSERVATION SYSTEM

T.E. Levens*, T. Bohl, U. Wehrle, CERN, Geneva, Switzerland

Abstract

Measurements of the bunch peak amplitude using the longitudinal wideband wall-current monitor are a vital tool used in the Large Hadron Collider (LHC) beam observation system. These peak-detected measurements can be used to diagnose bunch shape oscillations, for example coherent quadrupole oscillations, that occur at injection and during beam manipulations. Peak-detected Schottky diagnostics can also be used to obtain the synchrotron frequency distribution and other parameters from a bunched beam under stable conditions. For the LHC a beam-synchronous gated peak detector has been developed to allow individual bunches to be monitored without the influence of other bunches circulating in the machine. The requirement for the observation of both low intensity pilot bunches and high intensity bunches for physics requires a detector front-end with a high bandwidth and a large dynamic range while the usage for Schottky measurements requires low noise electronics. This paper will present the design of this detector system as well as initial results obtained during the 2012-2013 LHC run.

INTRODUCTION

In the Large Hadron Collider (LHC), peak-detection of the beam current signal from a longitudinal wall-current monitor (APWL) is a essential tool in the beam observation system. The measurement can be used to extract a number of parameters through both time-domain and frequency-domain analysis. One important use is the diagnosis of bunch shape oscillations, such as coherent quadrupole oscillations which can occur at injection or during beam manipulations. The peak-detected signal will show an instability as a variance in the peak amplitude of the bunch over many turns.

A second use of the signal is for "peak-detected Schottky", a technique developed by D. Boussard and T. Linnecar [1, 2] which has been used extensively in the SPS since the late eighties, especially during the operation as a $p\bar{p}$ collider. The theory of Schottky signals for both unbunched and bunched beams in the longitudinal and transverse planes is well developed [3–5]. In the case of an unbunched beam, the longitudinal Schottky spectrum gives the particle distribution in revolution frequency and therefore in momentum. For a bunched beam, information about the momentum spread (dispersion) can also be extracted in most cases [6]. Peak-detected Schottky is a special case for bunched beams using the longitudinal Schottky signal. It differs in that it uses only the peak amplitude of the beam current and results in a spectrum which, closer to that of an unbunched beam, provides information about the particle distribution in synchrotron frequency [7]. The deviation of the peak-detected Schottky spectrum from the synchrotron frequency distribution is mainly defined by the experimental set-up.

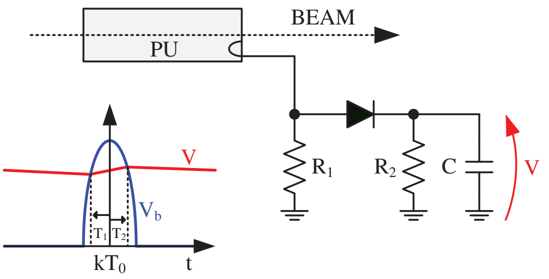

Figure 1: A simplified schematic of the peak-detector.

PEAK-DETECTOR

A simple circuit consisting of a fast switching diode and a capacitor detects the peak of the bunch current from a wideband pick-up as shown in Fig. 1. During the bunch passage, the diode is forward biased when $V_b > V$ (i.e. $-T_1 \leq t \leq T_2$) and the detector voltage can be found using the equation [8]

$$\frac{dV}{dt} = \frac{1}{\tau_1}(V_b - V) \tag{1}$$

where $\tau_1 = R_1R_2C/(R_1 + R_2) \approx R_1C$ and assuming $R_2 \gg R_1$. Equation 1 has a solution of the form

$$V(t) = \frac{1}{\tau_1}\int_{-T_1}^{t} V_b(t')e^{-(t-t')/\tau_1}dt' + V(-T_1)e^{-(t+T_1)/\tau_1} \tag{2}$$

Outside of the bunch passage, $V_b \approx 0$ and the diode is reverse biased. During this time, the decay of the detector voltage is given by the equation

$$\frac{dV}{dt} = -\frac{1}{\tau_2}V \tag{3}$$

where $\tau_2 = R_2C$. Similarly, the solution of Eq. 3 has the form

$$V(t) = V(T_2)e^{-(t-T_2)/\tau_2} \tag{4}$$

After a transient period, a quasi-stationary situation is reached and the variations of T_1 and T_2 are small and only defined by statistical fluctuations (Schottky noise). Then $V(T_1) \approx V(T_2)e^{T_0/\tau_2}$. Taking into account that $V(T_1) = V_b(T_1)$ and $V(T_2) = V_b(T_2)$ together with Eq. 2

---

[*] tom.levens@cern.ch

ISBN 978-3-95450-127-4

Table 1: Comparison of old and new peak-detector circuit values, time constants and simulated detector modulation index (h) when driven by a source with $h = 6\%$.

C	R_1	R_2	τ_1	τ_2	h
920 pF	50 Ω	1.0 MΩ	46 ns	920 μs	2.2%
120 pF	50 Ω	8.2 MΩ	6 ns	984 μs	6.7%

allows the stationary values of T_1 and T_2 to be found as functions of the beam parameters (e.g. bunch length for a given particle distribution) and experimental set-up (parameters τ_1 and τ_2).

DETECTOR OPTIMISATION

Initially the peak-detector used for many years in the SPS was adapted by scaling the time constant to match the LHC revolution frequency, as described in [8]. During the 2010 run, it was realised that this configuration gave less sensitivity than expected when comparing quadrupole oscillations measured with the peak-detector with ones obtained from turn-by-turn acquisitions with a 2.5 GHz oscilloscope.

Initial measurements of the detector were made using an amplitude-modulated pulse source. The pulse source was set to generate a bunch-like signal with a pulse length of 0.8 ns and this was modulated with a 80 Hz sinusoid. The test did not show a lack of sensitivity as the modulation index observed with the peak-detector matched well with that of the modulated source for a working point above 750 mV DC. At lower working points, the sensitivity was even found to increase which did not match the lack of sensitivity observed in the LHC. However, given that the charge in a circulating bunch is constant, it is clear that the quadrupole oscillations are better modelled as an modulation in both pulse amplitude and length, so that the integral $\int V(t)\,dt$ is constant.

A PSpice simulation was set up in order to test the variation due to the values of components R_2 and C and the DC working point of the diode whilst subject to combined pulse amplitude and length modulation. For each variable, two simulations were performed. In the first, the bunch length was increased by 13% and the amplitude decreased by 13%. In the second, the reverse was done. This represents the extreme values of a 6% modulation while keeping the enclosed charge constant. From the simulation, it was found that reducing C while increasing R_2 resulted in an increased sensitivity. A maximum value of R_2 was chosen to be 8.2 MΩ due to the practical constraints imposed by manufacturing the printed circuit board. The value of C was thus chosen to keep the decay time constant, τ_2, close to the original value of approximately 10 turns, as shown in Table 1. The simulation also agreed with the initial measurement in that at a lower DC working point the sensitivity was higher. Therefore a practical DC working point was chosen to be 0.5 V. The output of the modified diode detector is shown in Fig. 2 after a +6 dB output buffer.

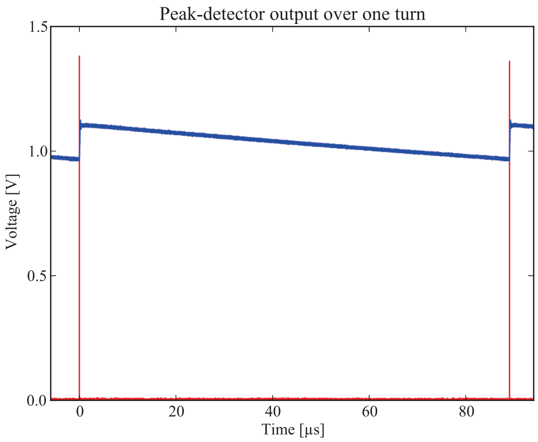

Figure 2: Measured output of the peak-detector over one turn of the LHC (89 μs).

HARDWARE DESIGN

RF Front-End

The front-end is defined as the signal chain from the output of the APWL pick-up to the diode detector, described in the previous section. Its purpose is to ensure a constant working point for the detector while allowing for a large dynamic range at output of the pick-up. In the LHC there is a difference of 34 dB signal level between a pilot bunch (2×10^9 protons) and the nominal physics beam (1×10^{11} protons). The usable frequency response of the APWL pick-up is 80 kHz to 3.5 GHz [9] and, in order not to overly distort the bunch shape seen by the detector, the front-end has been designed to be capable of this bandwidth with a good gain flatness.

In order to to allow a wide range of input signal levels, the front-end is built from a cascaded series of attenuation stages that can be inserted or bypassed using RF relays. The first three attenuation stages are built using 10 W power attenuators, switched with discreet coaxial relays, in an external chassis. The fourth stage, also in the external chassis, consists of a high-bandwidth RF amplifier in order to increase the signal level of low intensity bunches. A compromise between gain flatness and bandwidth had to be made when selecting the RF amplifier. The model chosen has good flatness of ±1.5 dB over the frequency range of 10 MHz to 2.5GHz. The amplifier will only be utilised for extremely low intensity bunches, as in most situations the output level from the APWL is sufficient to drive the diode detector directly. With the amplifier bypassed, the rest of the front-end signal has a frequency response of DC to above 3.5 GHz.

On the detector PCB, a binary sequence of four 1 W attenuators allows fine tuning of the detector voltage in steps of 1 dB. The attenuated signal is split using a resistive power divider to feed four detector channels. This allows four bunches circulating in the machine to be studied concurrently and independently. Three of the channels can

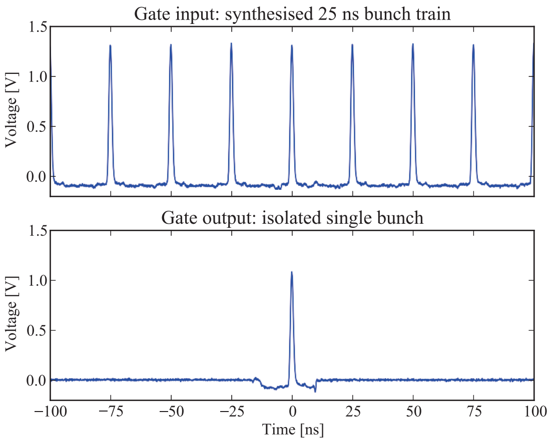

Figure 3: Gating of a single bunch in an synthesised 25 ns bunch train. The slight negative DC offset is due to the AC coupled output of the pulse generator.

also be bypassed to give 18 dB more signal into a single channel, intended for studies of a single, low intensity, pilot bunch.

Each detector channel has a high speed RF switch which can be toggled at the LHC bunch frequency of 40 MHz. With appropriate phasing, the switch allows the signal corresponding to a single bunch to be allowed through to the detector while masking the influence of the other circulating bunches. The action of the gate is shown in Fig. 3 where a single bunch is isolated from a 25 ns bunch train that has been synthesised using a pulse generator. Configuration of the phase of the gating signal will be critical and, due to the intended location of the peak-detector in the UX45 cavern, close to the beam line, access for manual set-up will not be possible. As the phase of the gating signal is fully remote controllable, an automatic system has been developed in order to detect when the bunch is correctly centred inside the gating pulse. A high speed comparator detects the bunch signal after the gate. By sweeping the phase of the gating signal, the usable range can be detected by observing the output of the comparator. Subsequently, the correct phasing to centre the bunch in the gate can be calculated.

Digital Card

The output from the detector channels are sampled by an ADC that is clocked by a bunch synchronous clock. If the sampling clock is not a harmonic of the revolution frequency (f_{rev}), there would be a jitter of the sampling point with respect to the peak-detector's output signal and this translates into additional noise in the value of the sampled signal. By using a harmonic of f_{rev} for the sampling clock, we can eliminate this additional noise source.

The sampled data is processed using a field programmable gate array (FPGA) which provides a variable rate decimation and low-pass filtering before storing the samples into memory. The card, shown in Fig. 4, is built for the custom VME-based crates that are used for the low-level RF of the LHC [10]. Control of the card, diagnostics and readout of the memory is via a 16-bit VME "P1" bus interface, while clocks and trigger pulses are provided by a custom "P2" backplane interface.

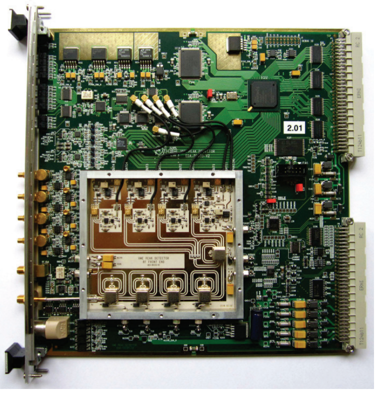

Figure 4: LHC peak-detector card in CERN's custom low-level RF VME form factor.

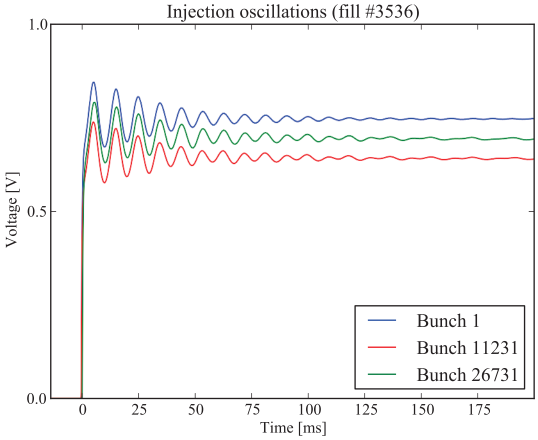

Figure 5: Injection oscillations of three selected bunches during injection of LHC fill #3536.

The card's on-board memory can store 512k samples per channel, giving a record length of 46.7 seconds when recording one point per turn. In addition to this, the memory is double buffered to allow continuous sampling with the VME front-end computer reading out from one buffer while the second is being written to.

RESULTS

Initial results were obtained with a prototype card towards the end of the first LHC run in February 2013. Injection oscillations have been measured with 200 ns trains of protons during LHC fill #3536. For this measurement, the first bunch of each injected batch was isolated using the gate. Selected bunches are shown in Fig. 5, from this we can measure the quadrupole oscillation frequency of 103.5 Hz, which is slightly less than $2f_s = 110.0$ Hz (for 6 MV RF at 450 MeV capture energy) due to the finite

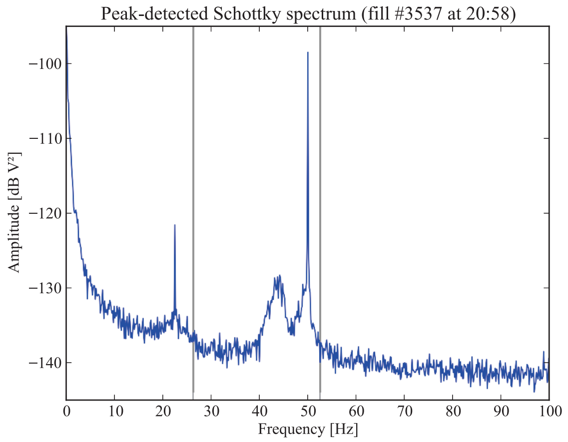

Figure 6: Longitudinal peak-detected Schottky spectrum from the recorded data. The grey lines mark the calculated synchrotron frequency $f_\mathrm{s} = 26.3$ Hz and harmonic $2f_\mathrm{s} = 52.6$ Hz.

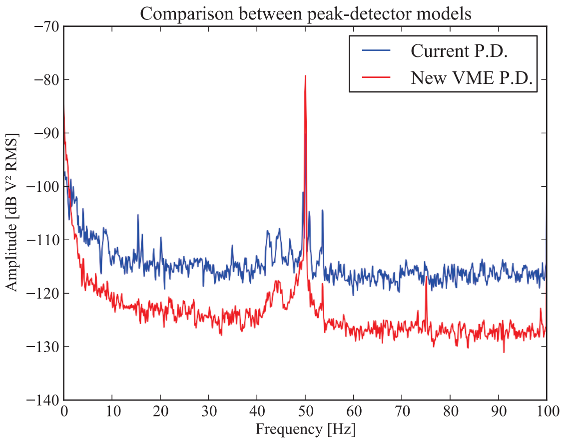

Figure 7: Comparison between old and new peak-detectors using a HP 3562A spectrum analyser.

bunch length. The damping time in the order of 100 ms also matches that observed during previous machine development sessions [11]. As each channel of the peak-detector can be individually gated on a specific bunch, and the readout of data is possible between the batch injections, the possibility of automatically recording the injection oscillations of four selected bunches in each batch injected into the LHC has already been foreseen.

Schottky measurements have also been made by taking a FFT of the time-domain sampled data, shown in Fig. 6. The distribution representing the second harmonic of the synchrotron tune can clearly be seen below the calculated value of $2f_\mathrm{s} = 52.6$ Hz (for 12 MV RF at 4 TeV flattop energy). The “dip” in the distribution around 46 Hz is not well understood but has been observed regularly in the LHC [12]. The spurious line due to the mains at 50 Hz is clearly visible. The line at 22.5 Hz has been observed in previous Schottky measurements made with beam two, but its source is not clear [12]. Measurements to compare the new peak-detector with the existing model were also made using a HP 3562A spectrum analyser, shown in Fig. 7. Although the relative noise floors in the two measurements are not representative, the detail of the $2f_\mathrm{s}$ spectrum is clearly more visible than with the previous peak-detector and, again, we can see the “dip” in the spectrum. The noise floor of the ADC in the prototype card was not optimised, and it is hoped to improve this further in the final version of the card.

CONCLUSION

A new peak-detector for the LHC beam-observation system has been designed. The new VME card offers a number of additional features the most important of which is gating to allow observation of individual bunches circulating in the machine without the influence of others. Full remote control and readout will enable automatic diagnostic measurements. Initial results obtained at the end of the first LHC run look promising, both for measuring injection oscillations and for peak-detected Schottky.

REFERENCES

[1] D. Boussard *et al.*, “SPS Improvement Reports No. 154, 162 & 167”, CERN, Geneva, 1979.

[2] T. Linnecar, T. Bohl, E. Shaposhnikova, J. Tückmantel, “Capture Losses Caused by Intensity Effects in the CERN SPS”, AIP Conf. Proc. Vol. 773, June 2005, p. 345.

[3] J. Borer *et al.*, “Non-destructive diagnostics of coasting beams with Schottky noise”, HEACC’74, Stanford, May 1974, p. 53.

[4] S. Chattopadhyay, “Some fundamental aspects of fluctuations and coherence in charged-particle beams in storage rings”, CERN, Geneva, Oct 1984, CERN-84-11.

[5] D. Boussard, “Schottky noise and beam transfer function diagnostics”, CAS, Oxford, Sep 1985, CERN-87-03, p. 416.

[6] V. Balbekov, S. Nagaitsev, “Longitudinal Schottky spectra of bunched beams”, EPAC’04, Lucerne, MOPLT109, 2004

[7] E. Shaposhnikova, “Longitudinal peak detected Schottky spectrum”, CERN, Geneva, Apr 2009, CERN-BE-2009-010.

[8] E. Shaposhnikova, T. Bohl, T. Linnecar, “Longitudinal Schottky spectrum of the peak bunch amplitude signal”, PAC’09, Vancouver, May 2009, TH5RFP038, p. 3531.

[9] T. Bohl and J.F. Malo, “The APWL Wideband Wall Current Monitor”, CERN, Geneva, Feb 2009, CERN-BE-2009-006.

[10] A. Butterworth, J. Molendijk, R. Sorokoletov, F. Weierud “Control of the low level RF system of the Large Hadron Collider” ICALEPCS’05, Geneva, Oct 2005.

[11] T. Mastoridis, P. Baudrenghien, “RF Observations during High Single Bunch Intensity MD”, CERN, Geneva, Feb 2012, CERN-ATS-Note-2012-023.

[12] T. Bohl, private communication.